

Solid Colloidal Particles Inducing Coalescence in Bitumen-in-Water Emulsions

J. Legrand,[†] M. Chamerois,[‡] F. Placin,[‡] J. E. Poirier,[‡] J. Bibette,[†] and F. Leal-Calderon^{*,§}

Laboratoire Colloïdes et Matériaux Divisés, ESPCI, 10 Rue Vauquelin, 75231 PARIS Cedex 05, France, COLAS, Laboratoire Central de Recherche, 4, Rue Jean Mermoz, 78771 Magny-les-Hameaux, France, and Laboratoire des Milieux Dispersés Alimentaires, ISTAB, Avenue des facultés, 33405 Talence, France

Received September 21, 2004. In Final Form: October 26, 2004

Silica particles are dispersed in the continuous phase of bitumen-in-water emulsions. The mixture remains dispersed in quiescent storage conditions. However, rapid destabilization occurs once a shear is applied. Observations under the microscope reveal that the bitumen droplets form a colloidal gel and coalesce upon application of a shear. We follow the kinetic evolution of the emulsions viscosity, η , at constant shear rate: η remains initially constant and exhibits a dramatic increase after a finite time, τ . We study the influence of various parameters on the evolution of τ : bitumen droplet size and volume fraction, silica diameter and concentration, shear rate, etc.

Introduction

Emulsions are widely used in a variety of applications because of their ability to transport or solubilize hydrophobic substances in a water continuous phase (e.g., painting, paper coating, road surfacing, lubrication, etc.). Emulsion technology drastically simplifies the pourability of many hydrophobic materials, which behave almost like solids at room temperature. For example, bitumen used for road surfacing is very difficult to handle at room temperature due to its extremely high viscosity ($> 10^5$ Pa s). The temperature has to be raised to ~ 150 °C in order to get sufficient fluidity. Instead, bitumen-in-water emulsions are quite easy to handle due to their low viscosity at room temperature. The main requirements of such emulsions are very good stability in storage conditions and rapid destabilization upon spreading on the road.

The irreversible destabilization of emulsions can be due to either coalescence¹ or Ostwald ripening.² When the two phases are poorly miscible, as is the case with bitumen and water, coarsening is only due to coalescence phenomena. Coalescence consists of the rupture of the thin liquid film between two adjacent droplets.³ Philip et al.⁴ have studied the coarsening mechanisms in liquid–liquid dispersions made of highly viscous oils such as bitumen (viscosity about 10^5 – 10^6 Pa s), in the absence of shear. When a destabilizing agent is added to the initially stable emulsion, a gel of partially coalesced droplets is rapidly formed. The gelation is followed by a contraction process that preserves the shape of the recipient and was termed “homothetic contraction”. Such a phenomenon is driven by surface tension and is analogous to the sintering process occurring during the densification of solid powders. In

the model experiments of Philip et al.,⁴ the destabilization was provoked by a chemical agent (NaOH) introduced in the continuous phase and the evolution was followed in quiescent conditions (no applied shear). In practical situations, bitumen-in-water emulsions are mixed with solid particles (from colloidal to macroscopic size) and that mixture is submitted to permanent agitation before deposition on the road surface. It is generally observed that the viscosity of the emulsion increases during the mixing process and that total separation of the water and bitumen phases occurs once the material is spread on a surface. In this paper, we examine the behavior in the laminar shear flow of a suspension comprising monodisperse bitumen droplets and solid silica particles with controlled specific surface area. We demonstrate that the presence of solid particles of colloidal size induces a destabilization of the emulsions once the shear is applied. We follow the evolution of the emulsions viscosity, η , at constant shear rate: η remains initially constant and dramatically increases after a finite time, τ . We study the influence of various parameters on the evolution of τ : bitumen droplet size and volume fraction, silica diameter and concentration, shear rate, etc. Our results are reminiscent of the shear-induced gelation observed in a wide variety of materials including emulsions of crystallized drops, hard sphere suspensions, cross linked polymers, etc.

Materials and Methods

Our emulsions are three-component suspensions consisting of dispersed bitumen oil, water as a continuous phase, and a surfactant partially adsorbed on the interface. We used SHELL bitumen with penetration grade 160/220 (the penetration grade is an indication of the fluidity obtained from the sinking of a needle in asphalt in normalized conditions) and with viscosity of the order of 10^5 Pa s at room temperature. Tetradecyl trimethylammonium bromide (TTAB, critical micellar concentration CMC = 3.5×10^{-3} M) purchased from Aldrich was used as surfactant to stabilize the emulsion. A crude emulsion was prepared by shearing a surfactant phase and bitumen at a temperature of 95 °C by means of a laboratory mixer (Heidolph, RZR 2041). The composition of the bitumen, TTAB, and water was 80:6:14 by weight. After the emulsification process, we obtained a polydisperse emulsion with a wide size distribution

* Author to whom correspondence should be addressed. E-mail: f.leal@istab.u-bordeaux1.fr.

[†] Laboratoire Colloïdes et Matériaux Divisés.

[‡] Laboratoire Central de Recherche.

[§] Laboratoire des Milieux Dispersés Alimentaires.

(1) Deminière, B.; Colin, A.; Leal-Calderon, F.; Bibette, J. *Phys. Rev. Lett.* **1999**, *82*, 229.

(2) Ostwald, W. Z. *Phys. Chem.* **1901**, *37*, 385.

(3) Kabalnov, A. S.; Wennerström, H. *Langmuir* **1996**, *12*, 276.

(4) Philip, J.; Poirier, J. E.; Bibette, J.; Leal-Calderon, F. *Langmuir* **2001**, *17*, 3545.

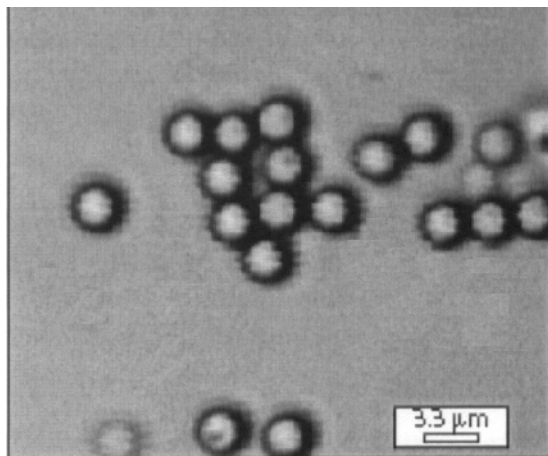


Figure 1. Laser scanning confocal microscopic image of a monodisperse emulsion with diameter $d_b = 2 \mu\text{m}$, obtained following the fractionated crystallization technique.

ranging from 0.1 to 10 μm . From the polydisperse emulsion, we get monodisperse fractions using a fractionation technique which is based on the liquid–solid phase transition induced by attractive depletion interactions.⁵ The fractionation method consists of introducing excess surfactant in the continuous phase. The large amount of surfactant micelles induces an attractive interaction (depletion forces) between the oil droplets due to the micellar osmotic pressure. Since the depletion force is proportional to the size ratio between the droplets and the micelles,⁶ it becomes possible to separate droplets of different sizes using a fractionated crystallization technique. The average droplet diameter was measured by means of quasi-elastic light scattering (Malvern CGS-3). Figure 1 shows a microscope image of an emulsion with droplet diameter $d_b = 2 \mu\text{m}$ resulting from the fractionation technique.

After the size-selection process, the continuous phase contains excess surfactant. To set the surfactant concentration at a fixed value, we centrifuged the emulsions four times, and each time, the continuous phase was replaced by a surfactant solution at a constant concentration of 2CMC. At that concentration, the emulsions were stable for several years in standard storage conditions ($T = 20^\circ\text{C}$).

Two different types of silica particles, Cabosil M-5 and Aerosil 130, purchased from Cabot Corporation and from Degussa, respectively, were used in this study. In the following, they will be termed P1 (Cabosil M-5) and P2 (Aerosil 130). Both types are combustion silica, and the average primary particle diameter is 250 nm for P1 and 16 nm for P2. The specific surface areas deduced from BET adsorption isotherms are $s = 200 \text{ m}^2/\text{g}$ for P1 and $s = 130 \text{ m}^2/\text{g}$ for P2. Despite their larger diameter, P1 particles possess a larger specific surface area because of their intrinsic porosity. Dispersions of the powders were prepared in pure water. Particles were partially flocculated in the aqueous phase and were sonicated using a high-intensity vibracell processor (Bioblock Scientific Vibracell) with a 0.3 cm head operating at 20 kHz for 2 min.

Each sample was prepared by mixing a mother bitumen emulsion and a silica dispersion. The compositional parameters characterizing the mixture are the mass fraction of the bitumen droplets, ϕ_b ($5\% \leq \phi_b \leq 20\%$), the mass fraction of the silica particles, ϕ_p ($0 \leq \phi_p \leq 0.5\%$), and the surfactant concentration, C ($1\text{CMC} \leq C \leq 4\text{CMC}$). We would like to emphasize here that C corresponds to the TTAB concentration initially introduced in the continuous phase. The total amount of surfactant molecules is the sum of the molecules present in the volume plus those adsorbed at the bitumen–water interface. Addition of silica particles causes a redistribution of the surfactant between the water volume and both silica and bitumen surfaces. We define the dimensionless parameter, θ , as the ratio between the total number of TTAB molecules (water volume + bitumen surface)

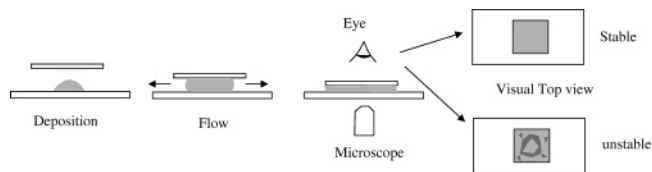


Figure 2. Scheme of the experiment performed to qualitatively assess the behavior of bitumen/silica mixtures under flow conditions.

and the maximum number of molecules that can be adsorbed on silica:

$$\theta \approx \frac{\Gamma_s}{2s\phi_p} \left[\frac{C \left(1 - \frac{\rho_e}{\rho_b} \phi_b \right) N_a}{\rho_e} + \frac{6\phi_b}{\rho_b d_b \Gamma_b} \right] \quad (1)$$

In eq 1, N_a is Avogadro's number, $\rho_e \approx 1 \text{ g/cm}^3$ is the average density of the emulsion, and $\rho_b = 1.03 \text{ g/cm}^3$ is the bitumen density. $\Gamma_s = 50 \text{ \AA}^2$ and $\Gamma_b = 150 \text{ \AA}^2$ are the surface areas occupied by TTAB molecules at the silica–water⁷ and bitumen–water⁸ interface, respectively. These values correspond to the maximum packing and were obtained after fixing the free surfactant concentration of the water phase above 1CMC. The factor 1/2 in the left-hand term of eq 1 is justified by the fact that TTAB forms a bilayer on the silica surface. The second term inside the brackets represents the number of surfactant molecules adsorbed on bitumen droplets, and we verified that this contribution is always smaller than 25% of the total surfactant amount. A value of θ significantly smaller than unity indicates that the adsorption capacity of silica particles is large compared to the total available surfactant. For P1 particles, assuming $d_b = 2 \mu\text{m}$, $\phi_b = 5\%$, $\phi_p = 0.5\%$, and $C = 1\text{CMC}$, we obtain $\theta = 0.5$; this rather low value indicates that silica particles may reduce the free surfactant concentration in the continuous phase below 1CMC due to their large specific surface area.

The qualitative behavior of the emulsions in the presence of silica particles was observed by means of a confocal laser scanning microscope (BX51WI-FV500 Olympus).

Emulsions were submitted to shear stability testing in a controlled strain RFSII rheometer (Rheometrics) using a Couette's cell with a gap of 0.25 mm. Since the emulsions become shear-sensitive in the presence of silica particles, we took all possible precautions in order to obtain reproducible data. To diminish the "preshear" when loading the samples, the emulsions were placed in the cell of the rheometer very carefully; the sample compression during loading was the lowest possible and was always done at the smallest rate. In a typical experiment, we first introduced the bitumen emulsion inside the cylindrical static pillar. Then, we carefully added the aqueous suspension containing silica particles. The two systems were manually mixed at very low rate in order to avoid any destabilization of the emulsion. Then, we took the rotor (internal bob) down at the lowest possible rate.

Results

1. General Behavior. The qualitative behavior of the system was explored following a very simple experiment. A drop (10 μL) of bitumen/silica mixture is deposited on a microscope glass slide. Then, a second slide (1 cm \times 1 cm) is carefully deposited in order to cover the sample: the slide weight forces the liquid to spread over approximately 1 cm, and the radial flow reveals the shear instability of the bitumen droplets (see Figure 2). The flow is interrupted after a few seconds, as soon as the liquid reaches the slide edges. The liquid confined between the two slides is brownish because of the light-absorbing properties of bitumen. If no silica particles are added, the

(5) Bibette, J. *J. Colloid Interface Sci.* **1991**, *147*, 474.

(6) Bibette, J.; Roux, D.; Pouligny, B. *J Phys. II (France)* **1992**, *2*, 401.

(7) Tanford, C. *J. Phys. Chem.* **1972**, *76*, 3020.

(8) Leal-Calderon, F.; Biais, J.; Bibette, J. *Colloids Surf., A* **1993**, *74*, 303.

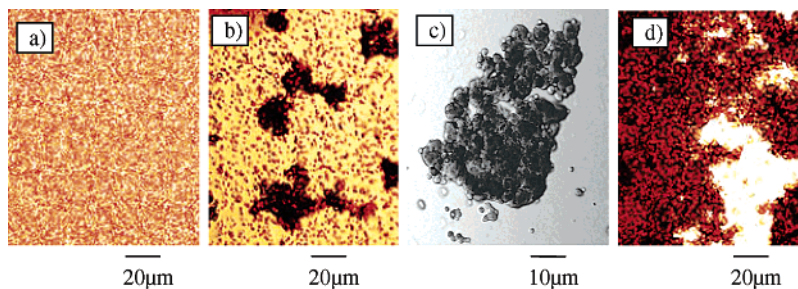


Figure 3. Microscopic images of bitumen emulsions submitted to the experiment described in Figure 2. $d_b = 2 \mu\text{m}$, $C = 1\text{CMC}$, and P1 particles. (a) $\phi_p = 0$, $\phi_b = 5\%$. (b) $\phi_p = 0.1\%$, $\phi_b = 5\%$. (c) $\phi_p = 0.1\%$, $\phi_b = 5\%$ (higher magnification). (d) $\phi_p = 0.1\%$, $\phi_b = 20\%$.

sample remains homogeneous at the macroscopic scale. However, some darker rings or spots appear in the presence of silica particles. From empirical considerations, it can be deduced that such rings or spots reveal the existence of zones where the bitumen concentration is larger than the average. The samples were observed under a microscope once the liquid reaches mechanical equilibrium, and some characteristic images have been reported in Figure 3. They were obtained with $d_b = 2 \mu\text{m}$ bitumen droplets at $C = 1\text{CMC}$. Figure 3a corresponds to the mother bitumen-in-water emulsion alone ($\phi_p = 0$) at $\phi_b = 5\%$. As expected, the emulsion is perfectly homogeneous and comprises individual Brownian droplets. This confirms the intrinsic stability of the system in storage conditions, as well as in flow conditions. Figure 3b was obtained in the presence of P1 particles at $\phi_p = 0.1\%$, $\phi_b = 5\%$, and $C = 1\text{CMC}$ after focusing the microscope objective on a darker zone; the presence of bitumen aggregates is clearly revealed. Figure 3c corresponds to the same system observed with an objective ensuring a higher level of magnification. The bitumen droplets are not only flocculated but they have also undergone partial coalescence. The shape relaxation occurs at the scale of several hours because of the extremely high viscosity of the bitumen phase.⁴ We verified that the clusters made of partially coalesced drops were not formed in the emulsion prior to its deposition between the two glass slides. Since their characteristic size is larger than $10 \mu\text{m}$, such clusters, if present, should have rapidly sedimented, forming a visible macroscopic phase. However, no sediment was observed at the scale of several hours. From the previous experiments, we deduce that bitumen emulsions become shear-sensitive in the presence of silica particles, meaning that they rapidly form clusters of partially coalesced drops.

Following the same procedure, we could qualitatively assess the impact of compositional parameters (ϕ_p , ϕ_b , C) on the extent of coalescence. The proportion of partially coalesced droplets increases with the particle mass fraction ϕ_p , all other parameters being constant. The surfactant concentration, C , also influences the shear sensitivity. For instance, the emulsion at $\phi_p = 0.5\%$, $\phi_b = 20\%$, and $C = 1\text{CMC}$ is substantially flocculated/coalesced. The proportion of coalesced droplets progressively decreases when C increases, until becoming negligible (no apparent flocculation/coalescence) for $C \geq 3\text{--}4\text{CMC}$. We did not measure the free surfactant concentration in the continuous phase. However, we observed that coalescence takes place preferentially when $C = \text{CMC}$ or when the parameter θ defined in eq 1 is significantly smaller than unity. For $\phi_p = 0.5\%$, $\phi_b = 20\%$, and $C = 1\text{CMC}$, we find $\theta = 0.4$ and the emulsion exhibits shear instability, as previously stated. Instead, $\theta = 2$ for $C = 4\text{CMC}$ and no coalescence was observed in this case. When $C \leq \text{CMC}$ or $\theta < 1$, it is likely that the free surfactant concentration in the water

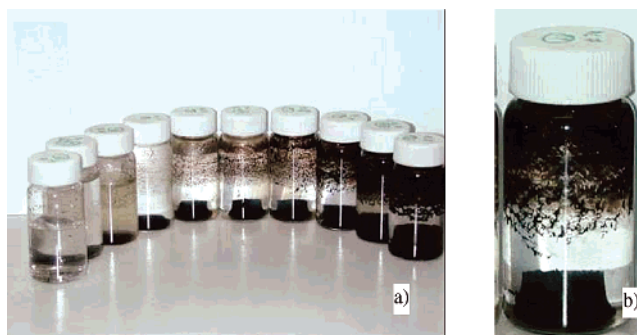


Figure 4. Final state of an emulsion vigorously shaken and stored at rest for several hours. (a) A collection of samples at the same initial bitumen fraction and variable ϕ_p values, increasing from left to right ($d_b = 2 \mu\text{m}$, $C = 1\text{CMC}$, $\phi_b = 10\%$, and P1 particles at $0 < \phi_p < 0.5\%$). Once the homothetic contraction was achieved, the water phase was removed and replaced by pure water in order to perfectly visualize coalesced bitumen. (b) The sample containing the largest amount of silica particles: most of the bitumen is localized at the bottom of the sample even if a small fraction wets the glass surface.

phase becomes lower than the CMC, a situation which is generally detrimental to emulsion stability.⁹

It appeared that the bitumen mass fraction has little influence on the shear instability within the explored range: $5\% \leq \phi_b \leq 20\%$. We only observed that the characteristic size of the clusters increases with ϕ_b . This is illustrated in Figure 3b and d that were obtained at the same C and ϕ_p values but at two different bitumen concentrations.

All of the above-reported observations can be reproduced at a larger scale. Samples containing bitumen/silica mixtures (total volume = 15 mL) were vigorously shaken for 10 s by means of a vibrating vortex-type mixer (Heidorf, Top-mix 94323). As could be expected, the intense flow created by the mixer is sufficient to induce rapid gelation of the samples. Immediately after this treatment, the emulsions are stored at rest, and phase separation occurs following the homothetic contraction phenomenon described by Philip et al.⁴ At the end of the process, a piece of almost pure bitumen lies at the bottom of the sample and the water phase remains brownish, meaning that it still contains bitumen in the dispersed state. Interestingly, we observed that the amount of residual bitumen in the water phase decreased with the solid particles content until the water phase became almost transparent above a threshold ϕ_p value of the order of 0.5% for $d_b = 2 \mu\text{m}$, $C = 1\text{CMC}$, $\phi_b = 10\%$, and P1 particles. Figure 4a shows a collection of samples at the same initial bitumen fraction ($\phi_b = 10\%$) and variable ϕ_p values, increasing from left to right. Once the homothetic contraction is achieved, the

(9) Bibette, J.; Morse, D. C.; Witten, T. A.; Weitz, D. A. *Phys. Rev. Lett.* **1992**, *69*, 2439.

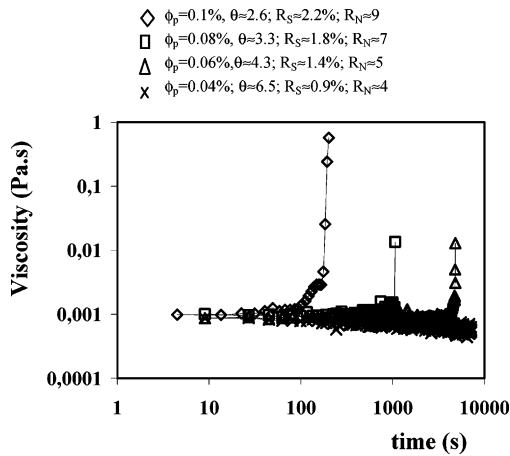


Figure 5. Evolution of the emulsion viscosity, η , under constant shear rate $\dot{\gamma} = 200 \text{ s}^{-1}$, in the presence of P1 particles. $d_b = 2 \mu\text{m}$, $\phi_b = 5\%$, $C = 1\text{CMC}$.

water phase was removed and replaced by pure water in order to perfectly visualize coalesced bitumen. It is clear in Figure 4a that the proportion of coalesced bitumen increases from left to right. Figure 4b shows the sample containing the largest amount of silica; most of the bitumen is localized at the bottom of the sample even if a small fraction wets the glass surface.

2. Shear Experiments. With the aim of characterizing the kinetics of the flow instability in perfectly defined conditions, the bitumen/silica mixtures were subjected to shear forces using a strain-controlled rheometer. We measured the evolution of the viscosity, η , as a function of time at a constant shear rate, $\dot{\gamma}$.

2.1. Influence of the Solid Particle Content. The typical behavior is illustrated in the curves reported in Figure 5, corresponding to the emulsion with $d_b = 2 \mu\text{m}$ bitumen droplets. The series was obtained at $\dot{\gamma} = 200 \text{ s}^{-1}$, $\phi_b = 5\%$, $C = 1\text{CMC}$, and variable ϕ_p ranging from 0.04% to 0.1%. For each curve, the viscosity is initially constant and close to that of the continuous phase due to the low bitumen content. After a finite time, η dramatically increases over at least one decade, reflecting a sudden gelation/destabilization of the system. A small amount of the sample was taken from the measuring cell in order to visualize the state of the gelled emulsion under microscope. We could observe the coexistence of Brownian drops and large interconnected clusters made of partially coalesced drops. We define the so-called gelation time, τ , as the time corresponding to the maximum value measured for the viscosity. The sudden jump offers a way to measure τ with sufficient accuracy. However, it should be noted that the viscosity measurements beyond the critical time, τ , were subject to a significant degree of experimental uncertainty and were not reported in Figure 5. We believe that the fluctuations in the viscosity measurements after τ may have at least two origins: (i) at irregular intervals, clumps of destabilized bitumen were observed to form between the rotating bob and the pillar of the rheometer cell. The clumps resulted from the progressive compaction of clusters under the effect of shear; (ii) the system was presumably exhibiting 'slip flow' once gelled.

It clearly appears in Figure 5 that the characteristic time at the onset of gelation decreases with the silica mass fraction. No gelation at all was observed below $\phi_p = 0.05\%$ after 10^4 s . The gelation time varies from approximately 4000 s at $\phi_p = 0.06\%$ to 200 s at $\phi_p = 0.1\%$. For $\phi_p > 0.2\%$, the instability occurred in less than 1 s and could not be measured with sufficient accuracy. In Figure 6, we plot

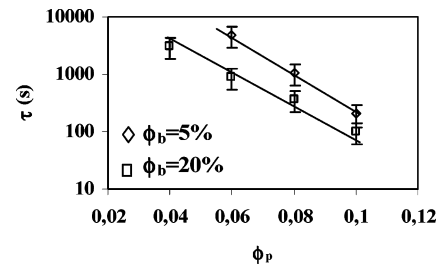


Figure 6. Evolution of the characteristic gelation time, τ , as a function of the mass fraction of P1 particles. $\dot{\gamma} = 200 \text{ s}^{-1}$, $d_b = 2 \mu\text{m}$, $C = 1\text{CMC}$. The solid lines are guides for the eyes.

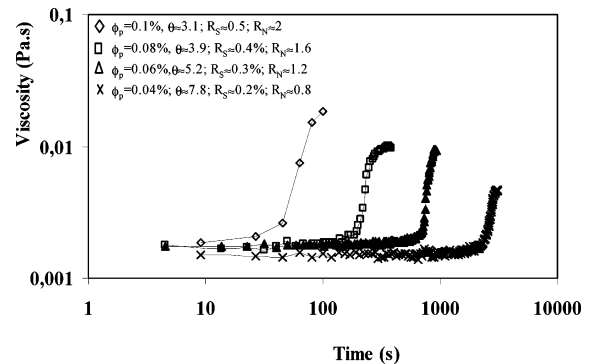


Figure 7. Evolution of the emulsion viscosity, η , under constant shear rate $\dot{\gamma} = 200 \text{ s}^{-1}$, in the presence of P1 particles. $d_b = 2 \mu\text{m}$, $\phi_b = 20\%$, $C = 1\text{CMC}$.

the evolution of τ deduced from Figure 5 (maximum value of the viscosity) as a function of ϕ_p . The curves reflect the strong influence of ϕ_p on the kinetics of the shear-instability since τ decreases over more than one decade while ϕ_p weakly varies from 0.06% to 0.1%.

2.2. Influence of the Bitumen Concentration. Similar measurements were performed within the above-described conditions except the bitumen concentration, which is now fixed at $\phi_b = 20\%$. The temporal evolutions of the viscosity are reported in Figure 7, and the characteristic τ value is determined from each plot. The curve τ vs ϕ_p at $\phi_b = 20\%$ is reported in Figure 6 together with the one previously obtained at $\phi_b = 5\%$. The two plots reveal the same qualitative evolution with comparable slopes. However, it is worth noting that, for the same ϕ_p , the gelation time is shorter for $\phi_b = 20\%$ than for $\phi_b = 5\%$. This tendency can be understood considering that gelation involves collisions between the drops. Since the emulsions are stable in quiescent storage conditions, it can be deduced that the process of aggregation followed by coalescence is activated, meaning that an energy barrier has to be overcome. At the working temperature ($T = 20 \text{ }^\circ\text{C}$), Brownian motion is insufficient to produce irreversible aggregation at the scale of several days. When submitted to a shear flow, the droplets experience collisions with sufficient energy to overcome the activation energy barrier, thus producing the observed gelation at a time scale ranging from seconds to hours depending on $\dot{\gamma}$. Collisions become more frequent as the droplet concentration increases, and consequently, the gelation process is accelerated.

2.3. Influence of the Shear Rate. We now examine the influence of the applied shear rate, $\dot{\gamma}$. In Figure 8 are plotted the kinetic curves, η vs. time, obtained for $C = 1\text{CMC}$, $\phi_b = 5\%$, and $\phi_p = 0.1\%$, with $\dot{\gamma}$ varying from 50 to 200 s^{-1} . The characteristic gelation time becomes shorter as $\dot{\gamma}$ increases. Again, this evolution can be understood within the frame of a collision-induced aggregation model. Increasing $\dot{\gamma}$ has the effect of raising the collision frequency

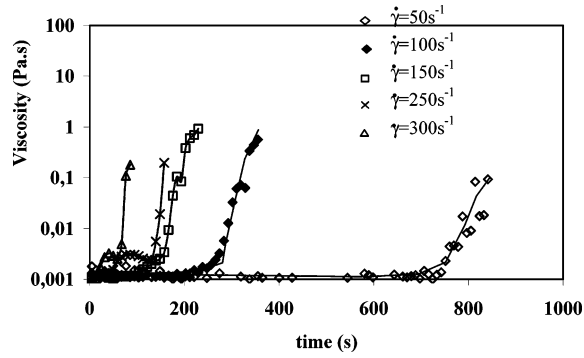


Figure 8. Evolution of the emulsion viscosity at variable shear rates, in the presence of P1 particles. $d_b = 2 \mu\text{m}$, $\phi_b = 5\%$, $\phi_p = 0.1\%$, $C = 1\text{CMC}$ ($\theta \approx 2.6$, $R_S \approx 2.2\%$, $R_N \approx 9$).

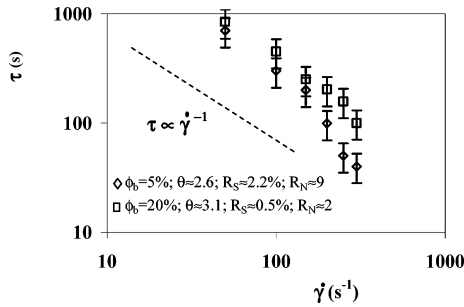


Figure 9. Evolution of the characteristic gelation time, τ , with shear rate, in the presence of P1 particles. $d_b = 2 \mu\text{m}$, $\phi_p = 0.1\%$, $C = 1\text{CMC}$. The dashed lines correspond to the scaling $\tau \propto \dot{\gamma}^{-1}$.

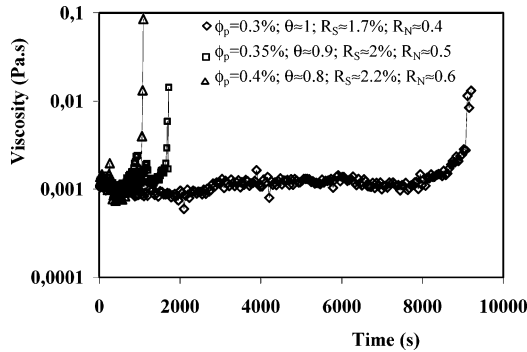


Figure 10. Evolution of the emulsion viscosity, η , under constant shear rate $\dot{\gamma} = 200 \text{ s}^{-1}$, in the presence of P1 particles. $d_b = 0.5 \mu\text{m}$, $\phi_b = 5\%$, $C = 1\text{CMC}$.

with the subsequent acceleration of the gelation process experimentally observed. The previous tendency is illustrated in Figure 9, where we report the evolution of τ as a function of $\dot{\gamma}$ in a log–log plot, for two bitumen volume fractions: $\phi_b = 5\%$ and $\phi_b = 20\%$. The data do not lie over a sufficient range to resolve the scaling law with good accuracy. However, we can estimate that the power-law exponent is close to -1 , in other words, the gelation time roughly varies as the inverse shear rate: $\tau \propto \dot{\gamma}^{-1}$.

2.4. Influence of the Bitumen Droplet Size. A second bitumen emulsion with droplet diameter $d_b = 0.5 \mu\text{m}$ was obtained through the size fractionation technique described in the experimental section (Materials and Methods). The emulsion becomes shear unstable in the presence of P1 particles within the experimental conditions previously described (see Figure 10; $C = 1\text{CMC}$, $\phi_b = 5\%$, $\dot{\gamma} = 200 \text{ s}^{-1}$). However, to obtain gelation times of the same magnitude (10^2 – 10^4 s), it was necessary to introduce a larger amount of silica particles compared to the case where $d_b = 2 \mu\text{m}$. It is interesting to note that, for a given gelation time, the silica mass fractions are approximately

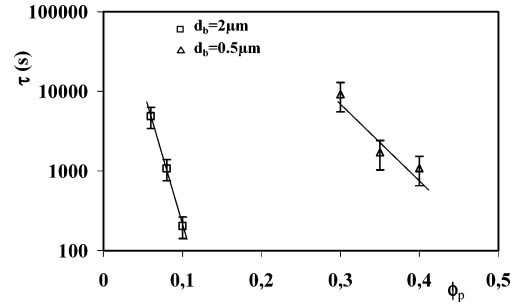


Figure 11. Evolution of the characteristic gelation time, τ , with the mass fraction of P1 particles. $\dot{\gamma} = 200 \text{ s}^{-1}$, $\phi_b = 5\%$, $C = 1\text{CMC}$. The solid lines are guides for the eyes.

in the same ratio as the inverse average diameters (Figure 11). For example, the solid content required to obtain $\tau \approx 1000 \text{ s}$ is equal to $\phi_{p1} \approx 0.07\%$ for $d_{b1} = 2 \mu\text{m}$ and is equal to $\phi_{p2} \approx 0.35\%$ for $d_{b2} = 0.5 \mu\text{m}$. These quantities verify the relation: $d_{b1}/d_{b2} \approx \phi_{p2}/\phi_{p1} \approx 4$ – 5 . This latter result strongly suggests that the specific surface area of the bitumen droplets, which is proportional to $1/d_b$, is a key parameter in controlling the gelation kinetics. The previous relation can be rewritten as $d_b \phi_{p2} = \text{constant}$, all other parameters being constant. In other words, the gelation time, τ , is at least partially determined by the quantity $d_b \phi_p$, which can be regarded as the amount of particles available per unit surface area of the bitumen droplets. To quantify more precisely this latter quantity, we define a new dimensionless ratio, R_S , as the total cross-sectional area of the primary silica particles ($N_p \pi d_p^2/4$, where d_p is the particle diameter and N_p is the total number of silica particles) divided by the total surface area of the bitumen droplets:

$$R_S \approx \frac{\rho_b d_b \phi_p \left(1 - \frac{\rho_e}{\rho_b} \phi_b\right)}{4 \rho_p d_p \phi_b} \quad (2)$$

where $\rho_s \approx 2.1 \text{ g/cm}^3$ is the silica density. In other words, R_S represents the maximum fraction of the bitumen surface that the silica particles could cover if they were deposited/adsorbed at the bitumen/water interface. For $\phi_b = 5\%$, $\phi_p = 0.07\%$, $d_p = 200 \text{ nm}$, $d_b = 2 \mu\text{m}$, eq 2 gives $R_S \approx 1.6 \times 10^{-2}$. Thus, when $\tau \approx 1000 \text{ s}$, the equatorial surface of the solid particles represents less than 2% of the total bitumen surface. It is also useful to define the dimensionless quantity, R_N , as the ratio between the total number of particles and bitumen droplets:

$$R_N \approx \frac{\rho_b d_b^3 \phi_p \left(1 - \frac{\rho_e}{\rho_b} \phi_b\right)}{\rho_p d_s^3 \phi_b} \quad (3)$$

In the conditions leading to $\tau \approx 1000 \text{ s}$, $R_N \approx 0.6$ for $d_b = 0.5 \mu\text{m}$ and $R_N \approx 7$ for $d_b = 2 \mu\text{m}$. Such low values underline the high destabilizing efficiency of P1 particles, since a relatively small amount of particles per bitumen droplet is sufficient to induce gelation under shear.

2.5. Influence of the Silica Particle Size. With the aim of probing the role of the particle size, a series of experiments was carried out in the presence of P2 particles. For the sake of comparison, the gelation times *versus* $\dot{\gamma}$ for P1 and P2 particles have been reported in Figure 12. They were obtained with the same bitumen emulsion $d_b = 2 \mu\text{m}$, in identical conditions: $C = \text{CMC}$, $\phi_p = 0.1\%$, and $\phi_b = 5\%$. For both systems, the scaling of τ with $\dot{\gamma}$ remains close to that previously reported: $\tau \propto \dot{\gamma}^{-1}$. The main

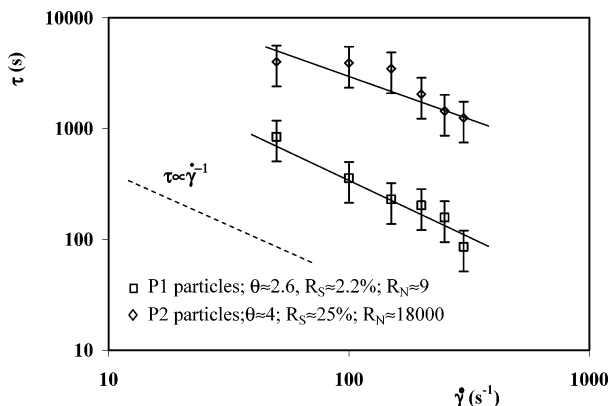


Figure 12. Evolution of the characteristic gelation time, τ , with shear rate, in the presence of P1 and P2 particles. $d_b = 2 \mu\text{m}$, $\phi_b = 0.1\%$, $C = 1\text{CMC}$, $\phi_b = 5\%$. The solid lines are guides for the eyes. The dashed lines correspond to the scaling $\tau \propto \dot{\gamma}^{-1}$.

experimental fact to underline is that the gelation times obtained for P2 are around half a decade larger than those obtained for P1. Following eqs 2 and 3, we get $R_S \approx 2 \times 10^{-2}$, $R_N \approx 10$ for P1 particles and $R_S \approx 0.25$, $R_N \approx 18\,000$ for P2 particles. Despite their larger number density (given by R_N) and larger coverage capacity (given by R_S), P2 particles do not produce rapid gelation compared to P1. However, it is clear that R_N and R_S numbers have to be handled with care since both types of particles were flocculated in the water phase, as indicated in the experimental section (Materials and Methods). Therefore, the dimensionless parameters should be calculated considering the effective floc size and volume fraction. Unfortunately, we could not measure these quantities since they strongly depend on the shear rate and on the concentration of free surfactant in the continuous phase.

Discussion

In principle, understanding the shear instability should require two types of information that account for two distinct phenomena. The first one concerns the microscopic mechanism of the instability: how do the droplets get connected? The second one concerns the growth scenario and kinetics of the clusters that form under shear.

From all the previous results and observations, we deduce that the gelation process is due to coalescence events that irreversibly connect the droplets. Usually, coalescence is viewed as a thermally activated process governed by the nucleation of a tiny molecular-sized hole in the films that further grows under the action of surface tension. In some particular cases, coalescence may be induced by mechanical instabilities.¹⁰ As an example, antifoams are very often solid particles dispersed in foaming solutions that emerge into the air–water interfaces. The soap films become unstable and break when their thickness is comparable to the size of the particles and when the contact angle between the liquid and the particles measured through the liquid phase is larger than 90° .¹¹ We believe that the silica particles used in our systems induce the same type of “antifoaming” instability. A repulsive electrostatic force exists between bitumen and silica because of the cationic surfactant adsorbed on both surfaces. Thus, the emergence of silica particles into the bitumen–water interface is an activated process occurring at very low rate when the surfaces are saturated by TTAB,

i.e. when the free surfactant concentration in the continuous phase is larger than 1CMC. In the experiments reported in Figures 5–12, the total surfactant concentration is kept constant at $C = 1\text{CMC}$, but it is likely that the free surfactant concentration in the continuous phase is lower because part of the molecules is adsorbed on silica. The adsorption ratios, θ , are indicated in the legend of each figure. If the free surfactant concentration falls below 1CMC, the surfactant coverage is lowered and the repulsive barrier between silica and bitumen decreases. In quiescent conditions, the emulsions remain dispersed, suggesting that Brownian motion is still insufficient to overcome the silica–bitumen repulsive barrier. Only the application of a shear at sufficient strain rate allows rapid emergence of the silica particles at the bitumen–water interface.

The gelation observed in bitumen/silica mixtures is analogous to the shear instability already described in emulsions comprising partially crystallized drops.^{12,13} Fat crystals in the oil droplets play a key role in destabilization of the emulsions under shear. The suggested partial coalescence mechanism requires some fat crystals to be protruding from the droplet surface. On approach of other droplets through application of shear forces, crystals can pierce the thin film between droplets. As soon as the crystal from one droplet touches the oil phase of another, partial coalescence occurs, with the crystal being better wetted by the oil than the water and a lipid bridge forming between the two droplets. The coalescence of droplets is incomplete or partial because the network of fat crystals within the droplets allows the identity of original droplets to be retained in the aggregates. Davies et al. have explored the shear stability of emulsions containing triglyceride crystals.¹³ Increasing stresses were applied to the samples, and the apparent viscosity of the emulsion was registered following each stress application. Shear-induced destabilization occurred very suddenly at a certain critical shear stress. Constant stress experiments were also carried out, and the authors observed a slow variation regime followed by a rapid increase in the viscosity, exactly as in our bitumen/silica mixtures. This type of behavior is not restricted to emulsions but has been observed in a large variety of systems where gelation is induced by different microscopic mechanisms under shear flow. Among them, we can mention the gelation of weakly attractive hard spheres¹⁴ or the gelling of polymer solutions in the presence of cross-linkers.¹⁵ Whatever the gelation mechanism is, the shear viscosity is initially weakly changing (induction period) and suddenly increases over several decades within a very short period of time.

The problem of aggregation in flowing suspensions in one of the fundamental problems in colloid science and has motivated several theoretical developments. If we consider the aggregation of dilute hard spheres, two regimes are usually distinguished. At the first stages, the process is dominated by doublet formation and involves collisions between two particles. At longer times, large clusters appear and each cluster can grow by the accretion of any other primary particle or cluster. Potanin¹⁴ argue that the evolution of the system can be correctly described considering that all the particles are combined into uniform aggregates of identical radius. In other words,

(12) Wastra, P. Physical principles of emulsion Science. In *Food structure and behaviour*; Blanshard, J. M. V., Lillford, P., Eds.; Academic Press: New York, 1987; pp 87–106.

(13) Davies, E.; Dickinson, E.; Bee, R. *Food Hydrocolloids* **2000**, *14*, 145.

(14) Potanin, A. A *J. Colloid Interface Sci.* **1990**, *145*, 140.

(15) Omari, A.; Chauveteau, G.; Tabary, R. *Colloids Surf., A* **2003**, *225*, 37.

(10) Garrett, P. R. *J. Colloid Interface Sci.* **1979**, *69*, 107.

(11) Garrett, P. R. *Defoaming: Theory and industrial application*; Surfactant Sciences Series 45; Marcel Dekker: New York, 1993; Chapter 1.

the most probable mechanism of aggregation is of hierarchical type and involves cluster–cluster aggregation.

Two limiting cases are usually considered: perikinetic aggregation (caused by Brownian motion) and orthokinetic aggregation (caused by medium flow). At very low shear rates, when the Peclet number, P_e , is much less than unity ($P_e = 3\pi\eta_c d^3 \dot{\gamma} / 4kT \ll 1$, where η_c is the viscosity of the continuous phase, d is the hard sphere diameter, and kT is the thermal energy), Brownian motion dominates the aggregation kinetics. Under these conditions, the aggregation rate is insensitive to the applied shear rate. As soon as the Peclet number becomes significantly higher than unity, i.e. when shear rate increases, the convection becomes the dominant transport mechanism. In this limit, the probability of a primary droplet to be captured by another given droplet per unit time is given by

$$J = \frac{\pi}{6} \alpha n_1 d^3 \dot{\gamma} = \alpha \phi \dot{\gamma}$$

where n_1 is the number of primary droplets per unit volume and $\phi = \pi d^3 n_1 / 6$ is the volume concentration of droplets. The parameter α has been introduced to take into account the capture efficiency. Numerical calculations predict a power law dependence of α with the applied shear rate: $\alpha \propto \dot{\gamma}^{-\epsilon}$, ϵ being a positive coefficient of the order of 0.2 for weakly attractive hard spheres.¹⁴ As a consequence, the doublet formation rate is expected to vary with the applied shear rate as

$$J \propto \dot{\gamma}^{0.8}$$

In the range of shear rates applied in our experiments ($\dot{\gamma} > 50 \text{ s}^{-1}$), the Peclet number for the bitumen droplets is always larger than unity: $P_e > 224$ for $d_b = 2 \mu\text{m}$ and $P_e > 3.5$ for $d_b = 0.5 \mu\text{m}$. Therefore, it can be admitted that convection dominates the aggregation kinetics. To compare our measurements with the previous aggregation model, we assume that τ is proportional to $1/J$. This approximation is justified since the longest period in the gelation process

(induction period) corresponds to doublet formation, the hierarchical growth ensuring rapid agglomeration of the clusters once the doublets have been formed. The power law exponent experimentally obtained for the evolution of τ with $\dot{\gamma}$ is close to -1 and is in agreement with the predicted value of -0.8 , within reasonable experimental uncertainty.

Conclusion

In this paper, we have examined the shear-induced gelation of bitumen-in-water emulsions in the presence of silica particles. The phenomenology that was described is quite general since we were able to reproduce the same instability by adding anionic polystyrene spheres (200 nm) and many other colloidal objects such as clays and carbon black particles. We believe our results at least partially explain the destabilization of bitumen emulsions in road surfacing applications. As was described in the Introduction, emulsions are mixed together with solid aggregates, and it is likely that the finest fractions identically produce gelation since the mixture is submitted to intense shaking before its deposition on the road. More generally, our results reveal a new route to achieve fast orthokinetic destabilization of an emulsion comprising highly viscous droplets by simply adding solid particles in the continuous phase. We also noticed that coalescence occurred preferentially with highly viscous droplets such as bitumen. Instead, neither coalescence nor gelation was observed for fluid droplets such as alkanes, fluid silicone, or even bitumen droplets at 90 °C (the bitumen viscosity decreases over 6 decades between 20 and 90 °C⁴). It should be within the scope of future work to understand the role of droplet viscosity in the destabilization process.

Acknowledgment. This work was financially supported by COLAS Company. The authors gratefully acknowledge G. Durand for fruitful discussions. We also acknowledge G. Ducouret (LCM-ESPCI) for the access to the RSII rheometer and L. Lemelle (LST-ENS Lyon) for the confocal laser scanning microscope images.

LA047649S